Toulouse School of Economics

Case Study:

Wind Turbines in France: Exploring the Past and Forecasting Optimal Placements

Authors:

Blanpied Anna

Bracque Vendrell Maria

Cossais Eva

Donati–Arranz Matthieu

Pinault Raphaël

Puech Cindy

Professors:

Dominique Haughton

Max Halford

Academic Year 2023–2024

DU Magistère d'Économiste Statisticien

Contents

1 Introduction

The use of wind energy can be seen as far back as 3000 years. Before the Industrial Revolution, wind energy was primarily harnessed through the use of windmills which directly converted wind into mechanical rotational energy. With the Industrial Revolution came the widespread use of coal and other fossil fuels that largely replaced wind energy as fossil fuels provided a more constant, reliable, and greater source of energy.

Despite the greatness of fossil fuels, they have a large negative environmental impact, particularly through atmospheric carbon emissions which lead to global warming. Therefore, over the past couple of decades, following the Kyoto Protocol (Japan, 1997), governments and social movements have been trying to reverse the trend by intensifying the use of renewable energies.

With the creation of generators, wind energy has emerged as one of the most promising technologies to address global challenges related to sustainable energy supply, greenhouse gas emissions reduction, and the transition to renewable energy sources. Indeed, wind turbines use an inexhaustible resource: the wind.

However, wind turbines are a very controversial topic due to their visual and sound impact. In addition, for this energy conversion to be truly effective, it is necessary to engage in thorough consideration and optimize the positioning of wind turbines across the French territory.

The major challenge lies in the need to increase the share of energy produced by wind turbines to meet the constantly growing energy demand of our modern societies. But, the equation is complex due to a crucial peculiarity of energy generated from renewable sources, such as wind turbines: it cannot be stored or sent far from the production source. Therefore, it is essential to achieve a distribution that ensures maximization of energy production while minimizing the storage and movement of this production. Moreover, this complex approach must take into account a multitude of factors, including the consideration of residential areas.

The objective of this project is to give an overview of the history of wind turbines in France and after to find potential locations for future wind turbine installations in France. To do so, we will first provide a historical overview of wind turbines in France. Then, we will delve into an analysis of both power capacity and generation from these turbines. And finally, we will determine the most promising sites by first predicting the potential energy generated by the wind farm based on its location, and then by narrow it down to locations close enough to urban areas to avoid electrical energy losses associated with transportation.

2 Contributions

René Fury and Daniel Joly (1995) [6] highlighted in their work that in general climate data is not fully exploited for various reasons. Firstly, the spatial resolution of available data is often limited, typically around 1 kilometer at best. This means that specific details at smaller scales may be lost, limiting the accuracy of analysis. Additionally, the temporal scale used for this data, often annual or monthly averages, may not be suitable for certain analytical needs, particularly for applications requiring finer resolution on a daily scale. In our paper, scales for extrapolation can be chosen, as small as you want, and we use daily data.

In their paper, S. Rehman, M. A. Baseer, and L. M. Alhems [12] made a computer tool to help pick the best places for wind farms in Saudi Arabia where wind power could be profitable. To achieve this, they gathered historical wind speed data from 46 locations across Saudi Arabia spanning 40 years. Using spatial interpolation techniques, they estimated wind speeds at locations where direct data was not available, creating a comprehensive wind map of the country.

We used a comparable approach in our study. What sets our research apart is that our model directly predicts the real value of wind speed, whereas their method involves reclassifying interpolated wind data into 9 categories. Additionally, while they focused on Saudi Arabia, our study is conducted using data from France.

A more recent study by Naveen Goutham, Bastien Alonzo, Aurore Dupré, Riwal Plougonven, Rebeca Doctors, Lishan Liao, Mathilde Mougeot, Aurélie Fischer, and Philippe Drobinski [11] also applies Machine Learning methods to predict wind speed. This paper is based on eight years of wind speed measurements from 2010 to 2017 collected from 171 stations across mainland France and Corsica.

Their models rely on 25 explanatory variables, including the atmospheric state at the station locations. Their most effective models are random forest and gradient boosting, achieving a mean square error (MSE) of 0.94 m/s.

Comparing with this existing literature, our XGBoost model achieves a slightly lower MSE of 0.90 m/s with fewer explanatory variables, but the methodology appears quite similar. This underscores the effectiveness of machine learning models, particularly XGBoost, in improving the accuracy of wind speed prediction in France. These findings contribute to optimizing the utilization of wind resources and decision-making in the renewable energy sector.

To conclude, an innovative approach that our paper proposes is the use of a machine learning model that require very little information to produce accurate predictions, making it an efficient and cost-effective solution for climate analysis and forecasting.

Finally, in contrast to many previous studies that often focus on a specific region of France or on the positioning of wind turbines at given locations, our paper takes a more holistic approach by identifying optimal locations at a national scale. This broader approach allows for a more comprehensive overview of deployment possibilities, which can lead to more informed decisions and more efficient utilization of wind resources at a country-wide level.

3 Wind Turbine Operation

Before delving into the analytical and predictive part of our study, let's have a general understanding of how wind turbine work. To understand the functioning of wind turbines, it is essential to delve into the process of converting the kinetic energy of the wind into electrical energy.

The core of wind turbine operation lies in harnessing the energy produced by the wind. The blades of the turbines, whose shape and inclination are designed to capture the kinetic energy of the wind most efficiently, are positioned at the top of a tower. When the wind blows on the blades, it exerts a force on them, causing them to rotate. This rotational movement is transmitted to a rotor located at the top of the tower.

The rotor is connected to a generator. As it turns, it rotates a copper coil in a magnetic field, generating an electric current. This current is then transmitted by cables from the turbine nacelle to a transformer located at the base of the tower, where the electrical voltage is adjusted to integrate it into the electrical grid.

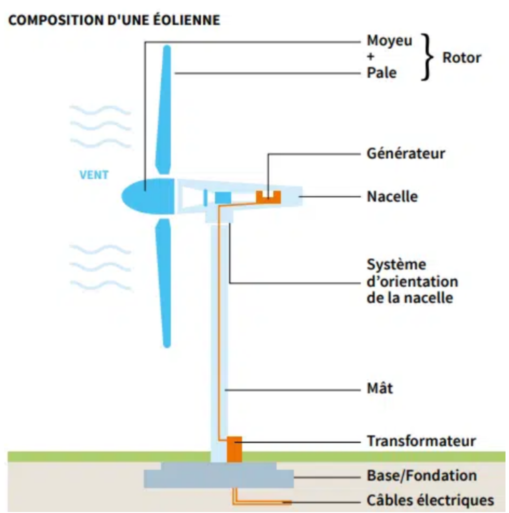

Figure 1: Operation of a wind turbine [14]

Wind, as a primary resource, plays a crucial role in the efficiency and profitability of these installations. Therefore, the first major consideration regarding the selection of sites for wind turbine installation is wind speed. Regions exposed to strong and consistent winds are preferred because higher wind speeds allow turbines to generate more energy. An essential aspect of the analysis is the diversity of winds throughout the year. Some locations may have a high average wind speed, but it is crucial that this speed remains constant to ensure a more reliable operation of the turbines.

To sum up, careful planning and a thorough understanding of wind characteristics in a given region are essential to maximize sustainable and efficient wind electricity production.

4 Overview of Wind Turbines in France

4.1 Historical Overview of Wind Turbines in France

The history of wind energy in France started with the introduction of the Darrieus turbine. The Darrieus turbine is a vertical-axis wind turbine, conceived by French inventor George Darrieus in 1931. Since then, a total of 20 916 MW (as date of December 31, 2022) of wind power capacity have been installed in France.

By the end of 2015, the total onshore installed capacity of 10,358 MW consisted of 5,956 turbines. According to figures released by the French government, there were nearly 2,000 wind farm installations across France by the end of 2019. While France has been a relatively late developer in wind power compared to other European countries, it has set the target of more than doubling onshore wind power capacity from 2015 levels by 2023. In February 2022, President Emmanuel Macron declared France's commitment to constructing 50 offshore wind farms, aiming for a cumulative capacity of at least 40 GW by 2050.

Additionally, the existing framework supporting renewable energy sources in France is based on Law No. 2015-992 dated 17 August 2015, titled "On Energy Transition for Green Growth". This legislation sets ambitious national energy goals. The PPE (Pluriannual Energy Program), updated by Decree No. 2020-456 on 21 April 2020, serves as a strategic roadmap for the French Government's energy initiatives over the next ten years. The primary objective is to guide France towards becoming a carbon-neutral nation by 2050. In 2023, according to the Ministère de la Transition Ecologique, renewable energies account for 20.7% of gross final energy consumption, and among renewable energies, wind power accounts for 11%.

4.2 Analysis of Wind Turbines in France

4.2.1 Wind Turbine Capacity

Data

Our data set contains all the terrestrial wind turbines in France, active or ordered. This data set is publicly available on a government website, Géorisques.gouv. The data set contains 11759 observations. We only kept the active windmills, which represent 7292 observations. There are in total 24 variables:

Variable	**Description**
id_aerogenerateur	Unique identifier for the wind turbine
id_parc	Unique identifier for the wind turbine park
code_insee	Code for the commune
nom_commune	Name of the commune
code_dept	Code for the department
code_reg	Code for the region
puissance	Power of the wind turbine
hauteur_totale	Total height of the wind turbine
hauteur_mat_nacelle	Height from base to nacelle
diametre_rotor	Rotor diameter
cote_ngf	Altitude above sea level
periode_allumage_lib	Lighting period (free text)
periode_allumage_desc	Description of the lighting period
type_feu_lib	Type of lighting (free text)
type_feu_desc	Description of the lighting type
date_mise_en_service	Date of commissioning
constructeur	Manufacturer of the wind turbine
reference_modele	Model reference
x_aerogenerateur	X-coordinate of the wind turbine
y_aerogenerateur	Y-coordinate of the wind turbine
epsg	EPSG code
libelle	Label
date_maj	Last update date
nom_eolienne	Name of the wind turbine

Table 1: Variables of the dataset on terrestrial wind turbines in France

We created four additional variables: *année* (the year the windmill was built), *latitude*, and *longitude* (the GPS coordinates), and *Région* (the region where the windmill is located).

Some observations required rectification as they had a power of 80MW, which seemed unusually high. In such cases, we conducted cross-referencing with other observations to obtain the correct values. To achieve this, we compared these suspicious windmills to others of the same model. If the model had only one power value in the data set, we assigned this value to the windmill. If there were multiple values, we first checked if there was another windmill of the same model from the same park. In such cases, we assigned the power value of the identified windmill to our suspicious windmill. If no such windmill was found, we examined windmills with similar characteristics (such as height, rotor diameter, and nacelle height) of the same model.

A few interesting graphs

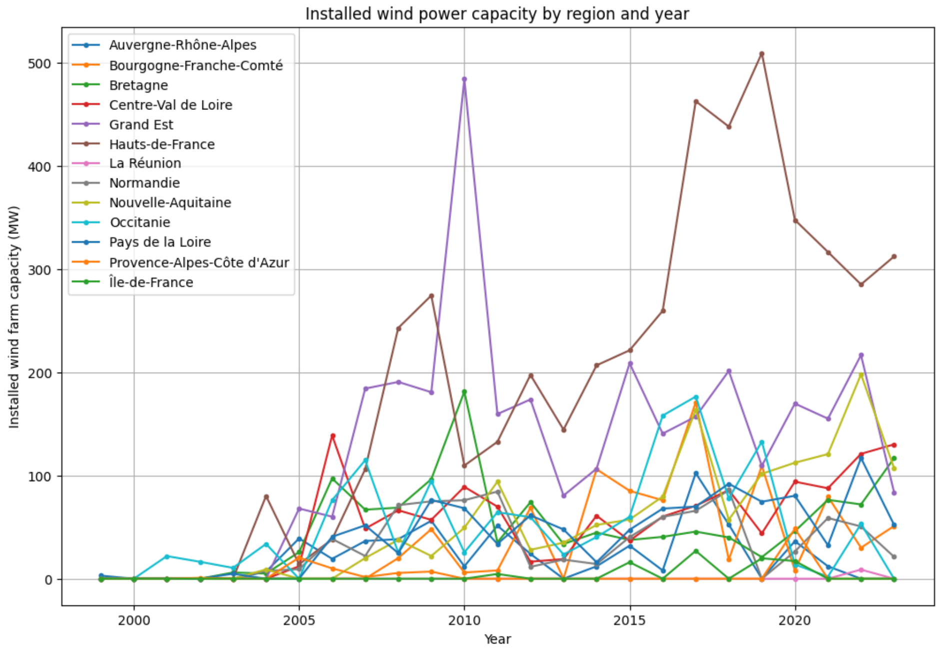

Figure 2: Installed wind power capacity by region and year

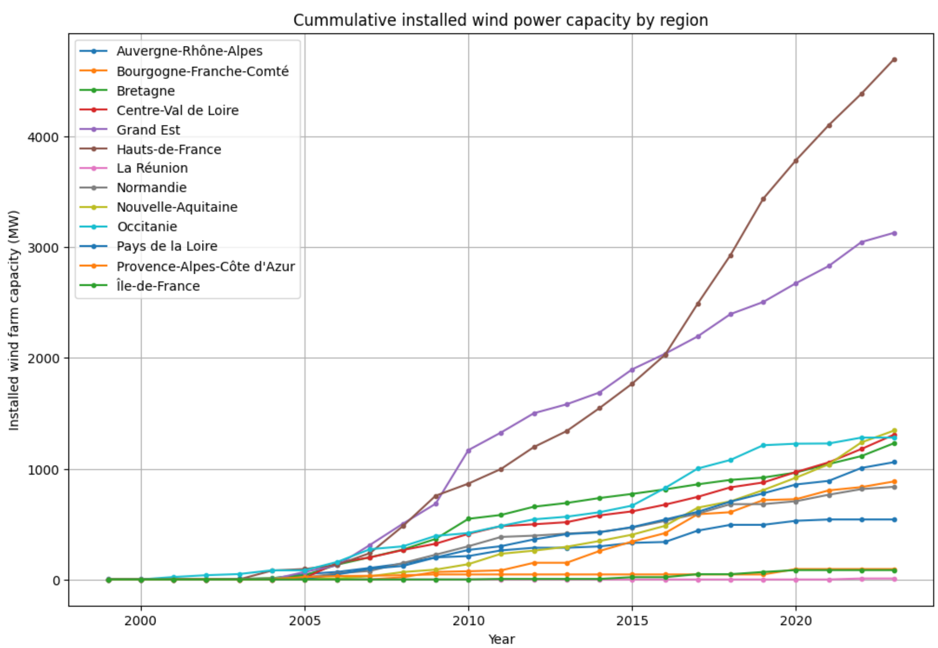

Figure 3: Cumulative installed wind power capacity by region

We can see that most of the regions have linear trends apart from "Haut-de-France" which has more of an exponential trend.

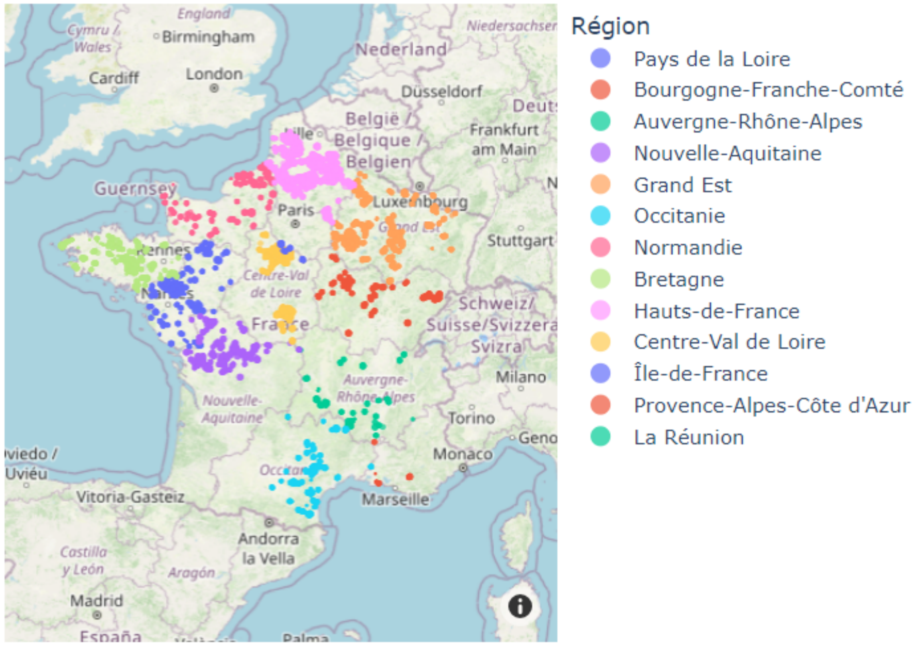

Figure 4: Map of the different wind farms in France

4.2.2 Wind Power Generation

Data

We use a data set from ODRÉ (OpenData Réseaux-Energies) for this section. This data set contains regional data from January 2013 from the éCO2mix application. éCO2mix is an easy-to-use tool created by RTE to help consumers better understand and consume electricity. It provides all electricity consumption and production indicators in real-time, 24 hours a day, at a national and regional level. Among other electricity production methods, it contains the level of energy production by wind turbines every 30 minutes by region.

Data cleaning

First, we deleted the columns that don't relate to wind turbines. After, we converted the 'Date' variable to a DateTime variable, and created three new columns with the month, the year, and the month and year that will be helpful in the future analysis. Finally, we deleted the 108 observations with missing values since we have 1 980 288 observations. The final variables of this data set are thus:

Variable	Description
Code INSEE région	Code for the commune
Région	Name of the region
Date	Energy production date
Heure	Energy production hour
Date - Heure	Energy production date and hour
Eolien (MW)	Energy production
Year	Energy production year
Month	Energy production month
month_year	Energy production year and month

Table 2: Variables of the data set on wind energy production in France

Data Analysis

First, let us have a look at the energy production of the different wind parks per region.

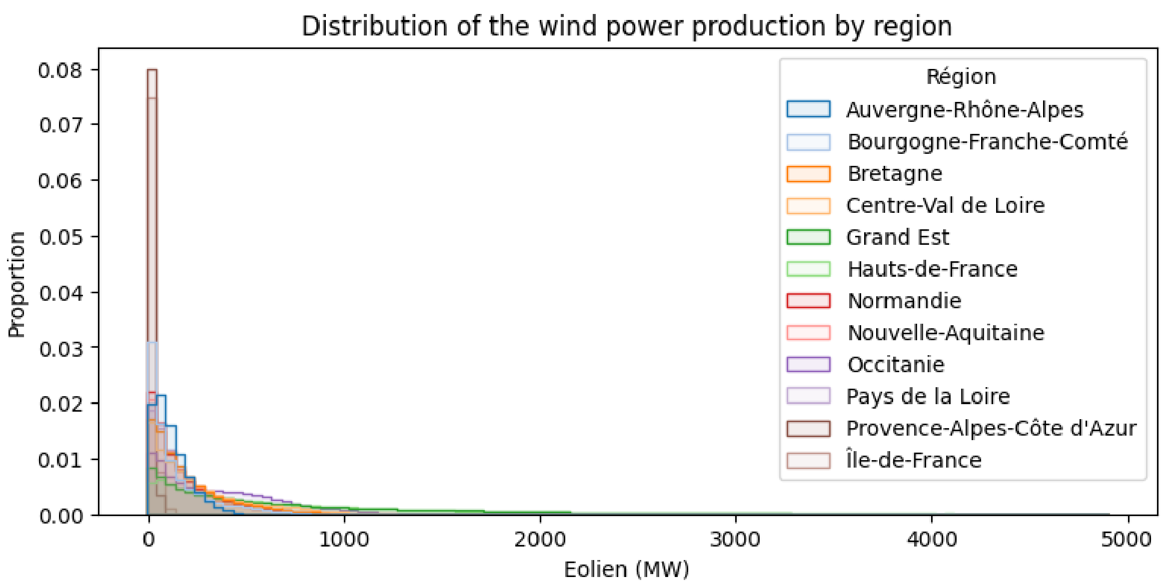

Figure 5: Distribution of the wind power production by region

We notice that overall, wind power generation follows a power law in each region. This means that the majority of observations are low production values, while high production values are rare. This could be due to various factors, such as the variability of weather conditions (e.g. wind speed and direction) that affect wind power generation. In addition, wind power generation capacity may vary according to the technology and infrastructure available in each region.

Then, we looked at the average production per day, month, and year for each region.

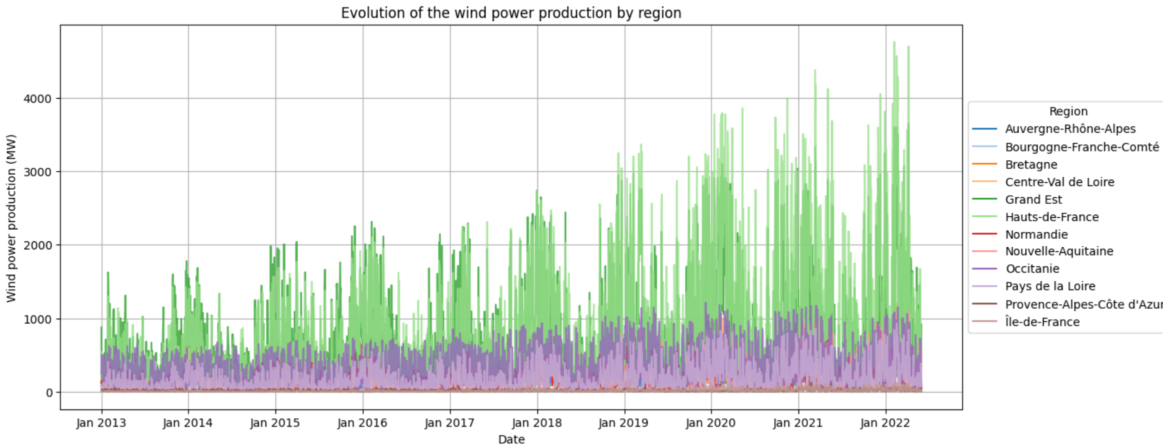

Figure 6: Evolution of the wind power production by region

We notice that it is a little hard to see all the regions on the same graph. However, we still notice that there is a kind of cyclicity that depends on the months of the year. This can also be seen in the following graph when we do not distinguish between regions.

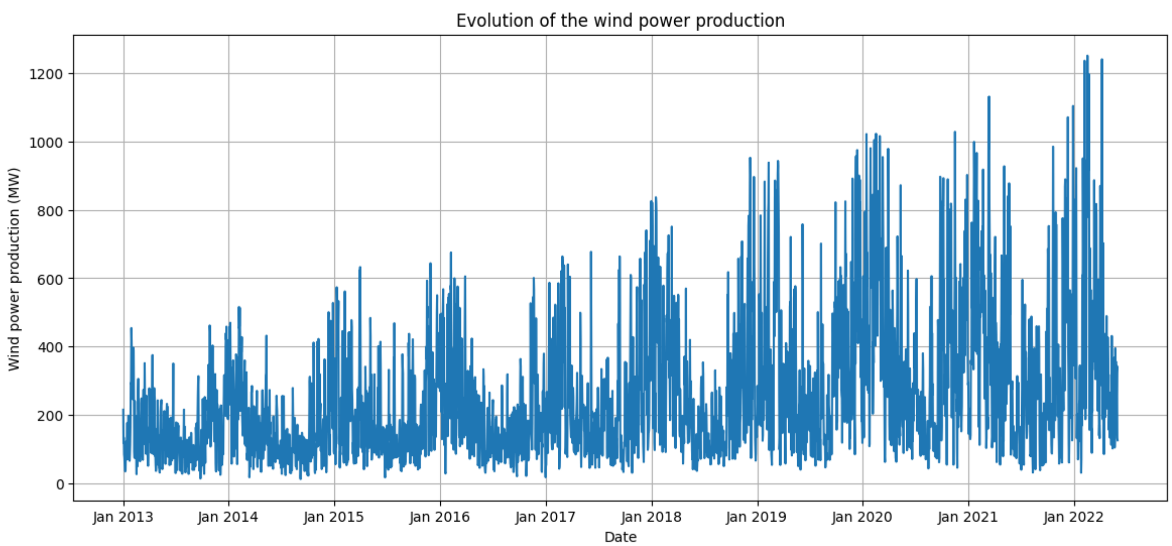

Figure 7: Evolution of the wind power production

To better visualize the cyclicity, and to take into account the difference in capacity between wind farms and years in each region, we're going to normalize the data. To do this, we need the capacity of wind turbines per region and year, we used the dataset from the previous section.

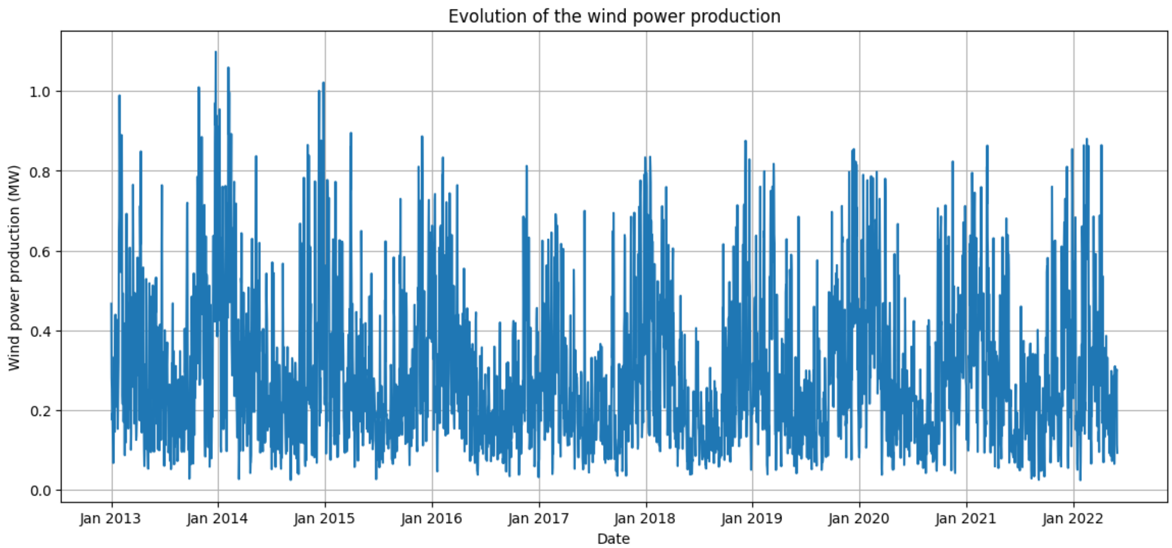

Figure 8: Evolution of the wind power production

We see that there is a cyclicity that depends on the months of the year. The production is higher during winter and lower during summer.

5 Wind Speed Prediction

5.1 Presentation of Data and Objectives

For this section, we chose to use the database of the Historical Meteorological Observation of France (SYNOP) [5]. This source contains meteorological and atmospheric data such as temperature, humidity, wind force, cloud description, visibility, and others. The data was collected by 62 stations spread across the French territory, with 42 located in metropolitan France. The period covered is from January 2018 to December 2022, with readings taken every 10 minutes, for which we have the average every 3 hours.

By applying physical formulas, extracted from scientific literature, detailed later in our study, to the wind speed obtained from our database, we can calculate the electricity production that a wind turbine could provide for each of these locations, at 3-hour intervals. By aggregating these results, we were able to evaluate the annual wind energy production for each of these sites.

Our initial database only covered 42 locations, corresponding to the 42 meteorological stations in metropolitan France. We chose to exclude the 2 stations located in Corsica to obtain more relevant results. By limiting ourselves to this data, our options for wind turbine placement were restricted to these specific 40 locations, thus excluding a part of the French territory from our study.

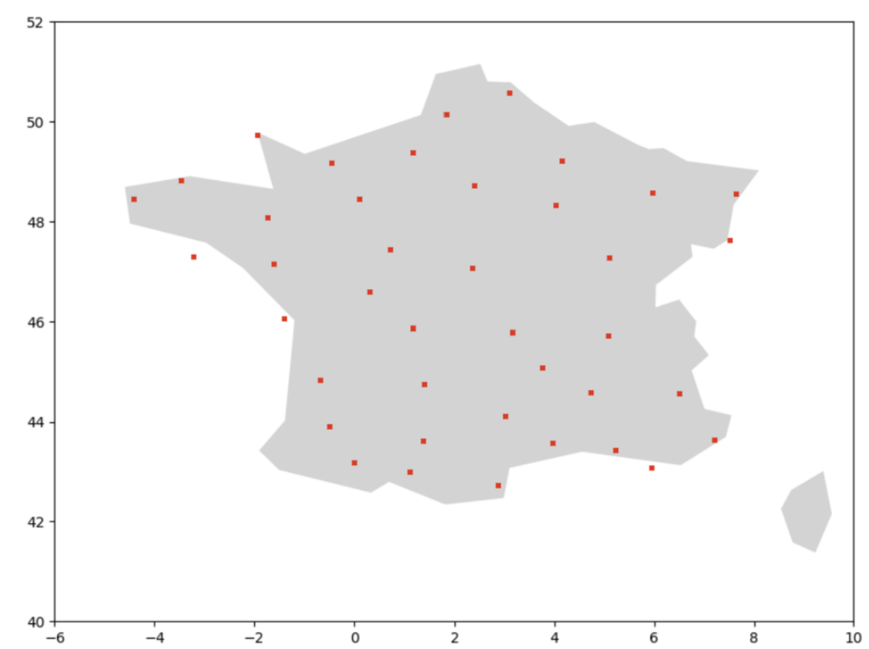

Figure 9: Position of the 40 meteorological stations used

This spatial limitation requires careful consideration when extrapolating our results to the national scale.

To realize wind speed prediction for optimizing wind turbine placements, we have worked on two solutions. The first solution involves implementing a statistical model, Kriging, which is particularly used in the context of spatial measurement estimation. The second solution is to develop a learning model using SYNOP data. In both cases, the models will be capable of predicting wind speed at a target location every day of the year, given only the GPS coordinates of the location, based on data from the 40 SYNOP stations.

And finally, to extend the application of these models to the entire French territory, we have adopted a grid-based approach. We divided France into squares of 10 km by 10 km, within which we estimated wind speed. This allowed us to then select the best locations for wind turbines, taking into account wind speed prediction, energy production calculation, and energy demand management by municipality.

5.2 Data Processing

It is important to remark that a wind turbine starts operating only when the wind speed reaches or exceeds 15 km/h, and it stops when the wind speed exceeds 90 km/h[3]. To ensure a more accurate evaluation of wind farm performance, we adopted a specific approach when aggregating data per day. Specifically, when the wind speed was not within the critical range of 15 to 90 km/h, we considered the wind turbine to not be moving and the data value to be zero. This strategy aims to exclude days where the daily average wind speed could theoretically fall within the operational range of wind turbines, yet the turbines were not operational during the day. By doing so, we obtained a more representative daily average of days for which the wind turbines had actually contributed to electricity production.

For example, let's imagine that the wind blew at a constant speed of 10 km/h all morning, but a storm occurred in the afternoon with gusts exceeding 90 km/h. In this case, the wind turbines would not have operated during the day. However, the average wind speed for that would have been around 50km/h, which falls within the speed range where a wind turbine can effectively operate.

5.3 Wind Speed Estimation: Kriging Approach

5.3.1 Theory

In the first approach, we use the Kriging approach. It is a statistical model popularized during the second half of the 20th century, particularly used in the context of spatial measurement estimation, notably in meteorology. This method aims to estimate atmospheric or geological data at a specific location based on various measurements made in the surrounding areas. Popularized by Georges Matheron, Kriging, named in honor of its creator, the geologist-statistician Danie Gerhardus Krige, remains widely used by many professionals in various sectors. This method is particularly useful when the measurement exhibits spatial correlation, offering the opportunity to fully leverage available spatial data.

Notation

Let Z be the random function characterizing the phenomenon we are trying to model, namely wind speed. We denote by p_0 the point in space for which we are trying to estimate the measurements, i.e., the values taken by Z at this point: Z(p_0). The objective is to estimate Z(p_0) based on the measurements made in the surrounding locations, where the different locations are denoted as $p_1, \ldots, p_N$ along with the observation distances (denoted as $d_{0,i}$ for the distance between point p_0 and p_i).

Definition and Assumption

We assume the intrinsic stationarity hypothesis, meaning that the statistical structure of the time series should remain relatively constant locally. This implies that, although the behavior of Z may exhibit trends, cycles, or patterns when observed on a global scale (across the entire map), these structures do not significantly change at smaller scales, i.e., locally. This assumption is key as it allows us to draw global conclusions from our estimates at a relatively local scale. In the context of wind estimation, this hypothesis has been confirmed by other studies [10].

Variogramme

To determine the relationship between the spatial distance of two points and the measurements of the evolution of the phenomenon of interest between these two points, we use a variogram. Graphically, the variogram can be represented by a scatter plot called variographic cloud.

The variogram is a function that encapsulates and synthesizes several key pieces of information in the study. Estimated from observations, it incorporates statistics of the observed phenomenon. Furthermore, indirectly through distances, it reflects the spatial autocorrelation of the data. On the x-axis, we have the spatial distance between two points in space, and on the y-axis, we have the differences in measurements associated with these two points. Analyzing the variogram allows us to estimate essential parameters for determining the weighting of neighboring observations when predicting unobserved values. Several types of variograms exist in the literature. We have chosen the spherical variogram due to its popularity and recommendations in the literature [10]. The parameters of the variogram are estimated from neighboring observations. Variograms are fitted using the method of maximum likelihood.

$$\textbf{Spherical Variogram :}\ \gamma(h) = \begin{cases} 0, & \text{si } h = 0 \\ \sigma^2 \left(1.5\frac{h}{a} - 0.5\left(\frac{h}{a}\right)^3\right), & \text{si } 0 < h \leq a \\ \sigma^2, & \text{si } h > a \end{cases}$$

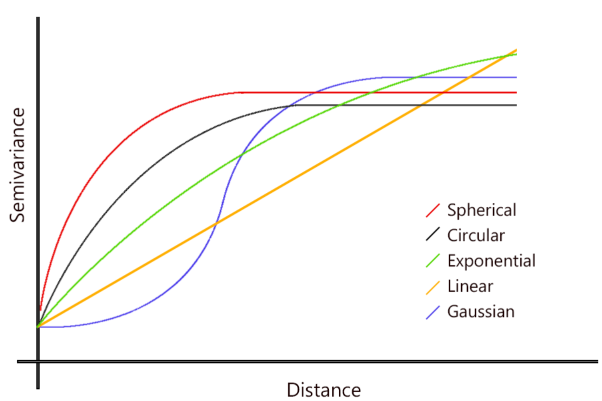

Figure 10: Commonly used variogram curves

Ordinary Kriging Method

The Ordinary Kriging method is based on the principle that the measurement to be estimated at a point p_0 is a weighted sum of the other retained actual measurements for the estimation: $Z_{ko}(p_0) = \sum_{i=1}^{N} \lambda_i Z(p_i)$. The weights λ_i must take into account the geographical distances between the points of study. The variogram is used to adjust the weight of each observation in the estimation according to its distance. In Ordinary Kriging, the estimation is obtained using the method of Lagrange multipliers, by imposing the constraint that the sum of the weights must be equal to 1.

Kriging Method with Linear Regression

The Kriging method with linear regression incorporates a linear regression component to an ordinary Kriging. The linear regression allows using variables that do not have spatial correlation in our estimation. More precisely, initially, we attempted to explain the phenomenon in question using variables that are not likely to be correlated with the geography present in our study. Then, we performed ordinary Kriging on the residuals obtained from linear regression. The Kriging part takes into account all variables that are likely to be correlated with space. It is recommended to use regression Kriging for this kind of study. [10].

To sum up, we can mention the summary presented by Floch (2013) [4] as follows: "Kriging provides an unbiased estimator, of minimal variance, which is also an exact interpolation since it returns for each known point an estimated value equal to the observed value."

5.3.2 Application

Following the recommendations of the literature, we performed estimations using the Regression Kriging model. We used the RegressionKriging function from the *pykrige.rk* package. The model trains and applies in a manner quite similar to other prediction models available in Python. In the linear regression part, we used indicator variables representing different days, months, and years to capture the cyclic trends of wind depending on the seasons [1]. Then, we explained the residuals, i.e., the part of the data not explained by the yearly seasons, using the wind speed from nearby actual meteorological stations. For the estimation with Kriging of wind speed at a point on the grid, we chose to retain the six closest stations.

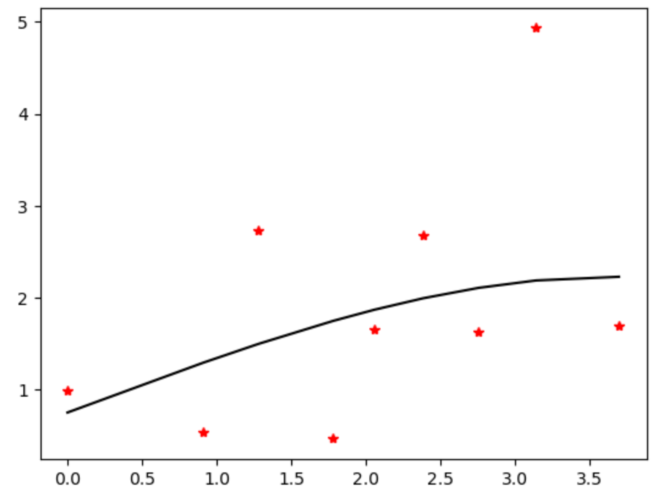

Figure 11: Variogram for the station at point (44.7,-0.60)

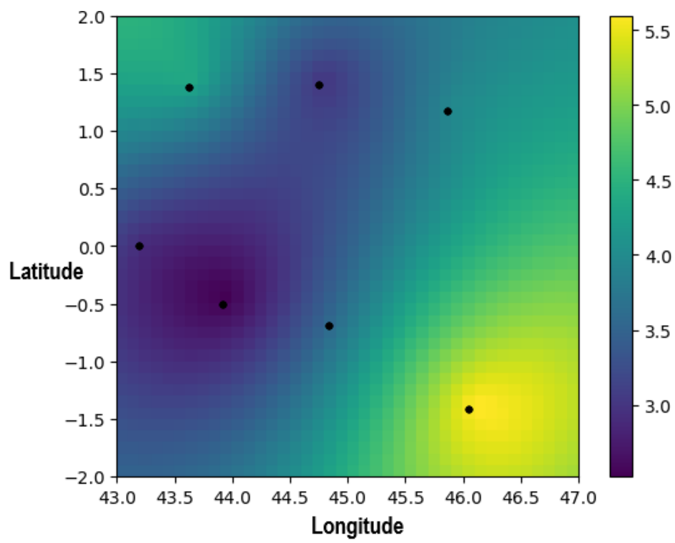

Figure 12: Estimation of wind speed for the station at point (44.7,-0.60) and its surroundings

The time required to train the model for the prediction of wind speed with grid points over a one-year period was approximately 15 minutes. The R^2 values for daily prediction varied between 0.3 and 0.5, depending on the region and the specific period selected during model training. Due to limited computing capacity, the Kriging model was trained on a partitioned database, thus restricting the training set to a specific time range and/or region of France. Hence, multiple R^2 performance results are obtained. For monthly prediction, R^2 values ranged between 0.8 and 0.85.

We appreciated the interpretability of the model, its renown in the literature, and its ability to distinguish the portion of the phenomenon explained by variables correlated to space from the ones related to time. This model has been validated by numerous instances and domain specialists, thus reinforcing the credibility of its results. However, in our case, the accuracy and predictive power of this model remain relatively low when focusing on daily predictions. Additionally, the model based on monthly prediction does not address our problem statement. Therefore, we choose not to consider it further. It would have been enriching to integrate other atmospheric data influencing wind speed, such as humidity or temperature.

With the goal of improving our model, we planed to explore new approaches, particularly those based on machine learning techniques, to obtain a more performant model that would offer more precision and relevant predictions for our specific context.

5.4 Estimation of Wind Speed: Machine Learning Approach

5.4.1 Linear Regression

To predict the wind at a location in France, we conducted a linear regression where our dependent variable is the wind speed. The explanatory variables considered include geographic variables, namely longitude, latitude, and altitude, which can capture the geographical characteristics of a region. For example, the proximity of oceans or mountains can have a significant impact on wind dynamics. We also introduced temporal variables with indicators for the year, month, day, and hour of the observation to capture seasonal and annual variability. Our model, presented below, is limited to the use of these variables to allow its application to any GPS point in France where only latitude, longitude, and altitude data are available.

$$\begin{aligned} Vitesse = \beta_0 + \beta_1 \cdot \text{Longitude} + \beta_2 \cdot \text{Latitude} + \beta_3 \cdot \text{Altitude} + \sum_{i=2019}^{2022} \beta_{4i} \cdot \mathbb{1}(\text{Année}) \\ + \sum_{i=2}^{12} \beta_{5i} \cdot \mathbb{1}(\text{Mois}_i) + \sum_{i=2}^{31} \beta_{6i} \cdot \mathbb{1}(\text{Jour}_i) + \sum_{i=1}^{23} \beta_{7i} \cdot \mathbb{1}(\text{Heure}_i) + \epsilon_i \end{aligned} \tag{1}$$

This linear regression, performed using the LinearRegression() function, yields negative and significant coefficients for the altitude and longitude variables (see Annex B). This means that the higher a point is in altitude, the weaker the wind speed. Similarly, the higher the longitude (i.e., the further east it is), the weaker the wind speed. The coefficient associated with the latitude variable is positive and significant, indicating that the higher the latitude (i.e., the further north it is), the stronger the wind speed.

Furthermore, the temporal variables seem relevant in the model as the majority of coefficients associated with the month and year indicators are significant, indicating notable seasonal and annual variations in wind speed. Similarly, the coefficients associated with the day and hour indicators are mostly significant, indicating an impact of the day of the month and the time of day on wind speed.

The results of this model highlight its limited performance. The coefficient of determination is 0.102, meaning that only 10% of the variance in wind speed is explained by the independent variables. The mean squared error is 6.18, indicating that on average, the squares of the differences between predicted and actual values are around 6 m/s (approximately 22 km/h). As seen in the figure below, this model does not seem to be sufficiently robust to capture the complexity of the relationships between variables for predicting wind speed. Additionally, it is observed that no predicted wind speed values exceed 7 m/s.

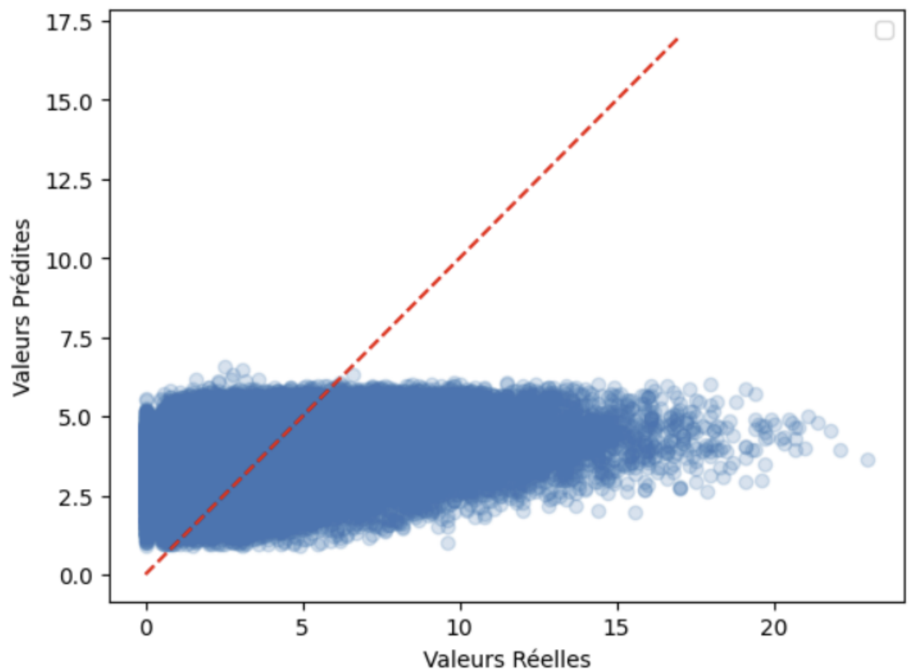

Figure 13: Comparison between the actual values and the predicted values by the linear regression

5.4.2 XGBoost

The results from the previous model being inconclusive, we proceeded with a second Machine Learning model: the XGBoost model.

XGBoost, or "eXtreme Gradient Boosting," is a machine learning algorithm that operates by iteratively constructing simple predictive models, called decision trees, and combining them sequentially. At each step, the algorithm identifies previous prediction errors and assigns increased weight to misclassified observations, allowing it to focus on areas of the dataset that need improvement.

With this new model, we seek to predict wind speed at a station using wind speed data from surrounding stations, taking into account the distance between them.

The coefficient of determination, R^2, obtained on the test dataset reaches a value of 0.80, which indicates the significant performance of this model. This value demonstrates the quality of the model's fit to the test data, making it a robust and reliable choice for predicting daily wind speed at the target station. Additionally, the mean squared error is 0.90, which means that on average, the squares of the differences between the predicted values and the actual values are around 0.90 m/s, equivalent to 4 km/h. The drawback of this model remains its interpretability. It is challenging to distinguish the role of each variable in this model. Therefore, we cannot provide further details on the results obtained. However, it is noted that the model tends to underestimate wind speed when it is high.

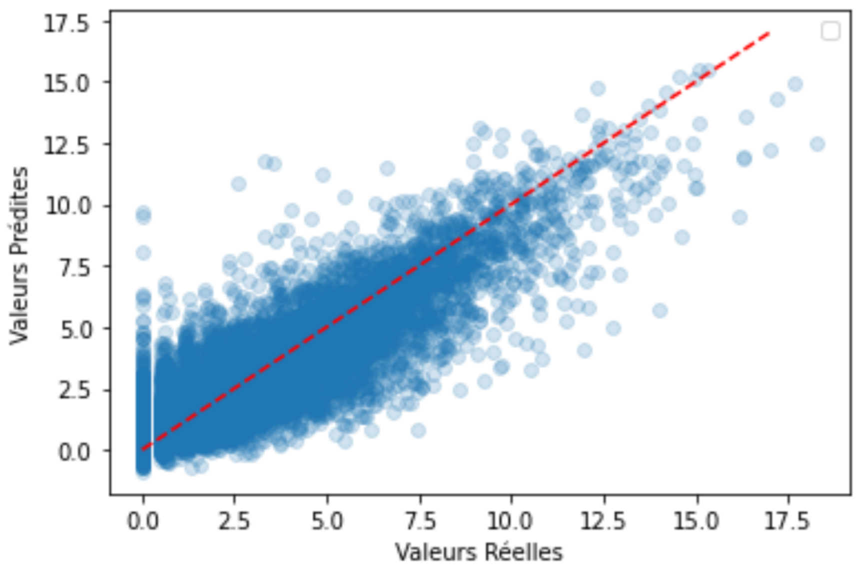

Figure 14: Comparison between the actual values and the predicted values by the XGBoost model

6 Location Selection

6.1 Extrapolation of Wind Speeds

Once our model is validated, it is necessary to estimate the wind speed at various locations in France to determine the optimal sites. As a reminder, our goal is to estimate the wind speed at a given location every day of the year over a one-year period. Due to our limitation in computing power and time, continuous estimation in space is not feasible. Moreover, a study on sparsely located points on the map could compromise the validity of our conclusions. Therefore, finding a balance is essential.

First, we created a grid covering the entire France, with a mesh resolution of 10 kilometers to extrapolate our model to different points. We wanted the grid to cover the entire metropolitan France, excluding Corsica. To achieve this, we calculated the length (respectively width) of France using the two farthest points from each other in latitude (respectively longitude). The distances are expressed in degrees (1 degree is approximately equivalent to 111 kilometers, this equivalence varies depending on our position on the Earth). Our goal was to make wind speed predictions at intervals of 10 kilometers (approximately 0.136 degrees). The number of points on the width (respectively the height) of the grid is naturally obtained by dividing the width (respectively the height) of France in degrees by the size of the grid mesh, which is 0.136.

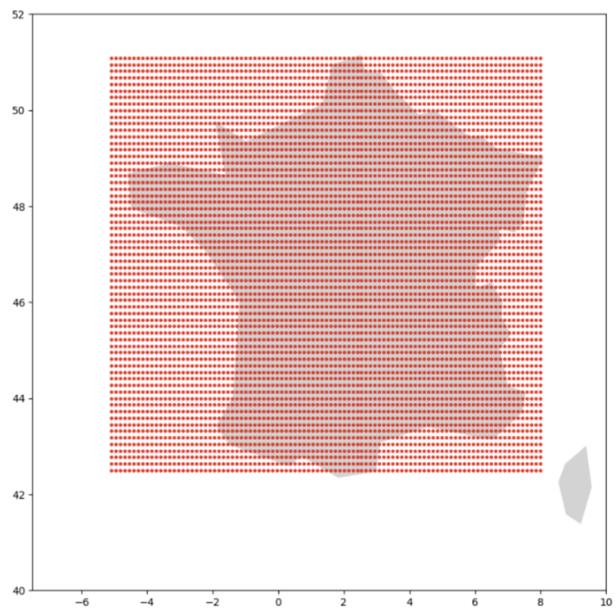

Figure 15: Representation of our grid

To bring our results closer to reality, we had to adapt this rectangular grid to the shape of France by excluding points located in the sea or in neighboring countries. For this purpose, we used the *sjoin* function to perform a spatial join between the points of our grid and the points within metropolitan France, defined by a *geopandas* dataset. We obtained the map below.

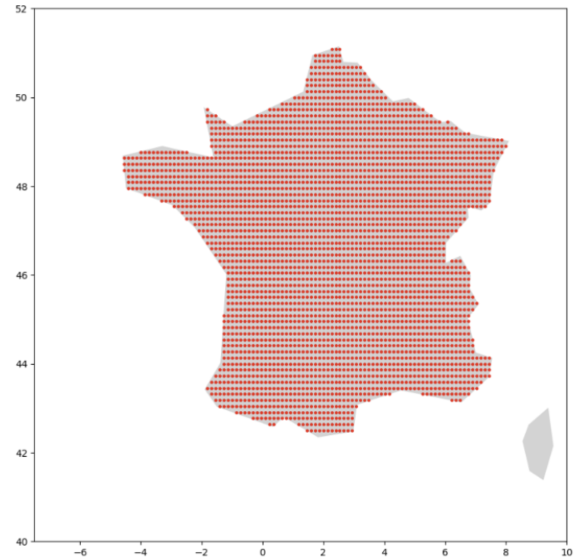

Figure 16: Representation of our grid limited to the borders of France

6.2 Integration of Residential Areas

After, we decided to exclude points that were located near major cities. We wanted to avoid to have wind turbines located too close to residential areas. By doing so, we sought to minimize the noise nuisances associated with their operation, preserve the aesthetic of the urban landscape, and comply with local regulations that may impose minimum distances between wind turbines and inhabited areas. Indeed, according to the Senate session of January 3, 2022, the distance between a wind turbine and a residential home must be at least 500 meters [13].

We decided to exclude cities having a population of more than 10,000 inhabitants, conciding them as major cities. To do so, we used a government API [7] that allowed us to retrieve information about all French municipalities, including their GPS coordinates and population, in *json* format.

Since our database is limited to the position of municipalities and not individual residences, we chose to impose a distance of 20 km between future wind turbines and municipalities with more than 10,000 inhabitants, which represents 1,042 municipalities in metropolitan France. We used the *cdsit* function of the *spicy* library to eliminate points located within a distance of less than 20 km from these municipalities, as showed on the map below. Finally, we obtained a database of 1892 potential locations with their latitude and longitude.

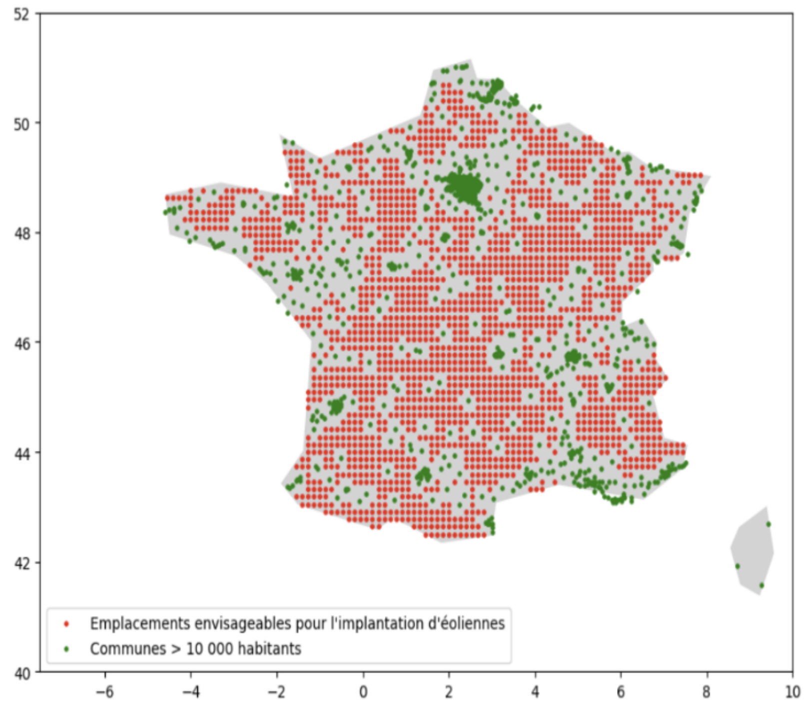

Figure 17: Representation of our grid with consideration of major cities

6.3 Wind Prediction

By applying the XGBoost model to the grid, we obtained a dataset containing wind speed predictions for the 1892 possible locations of wind turbines (corresponding to the red points on the previous map), for each day of the year.

We aggregated the results found by year to obtain an annual average of wind speed across different regions of France. By visualizing these aggregated data, we can identify areas that have optimal conditions to maximize wind energy production.

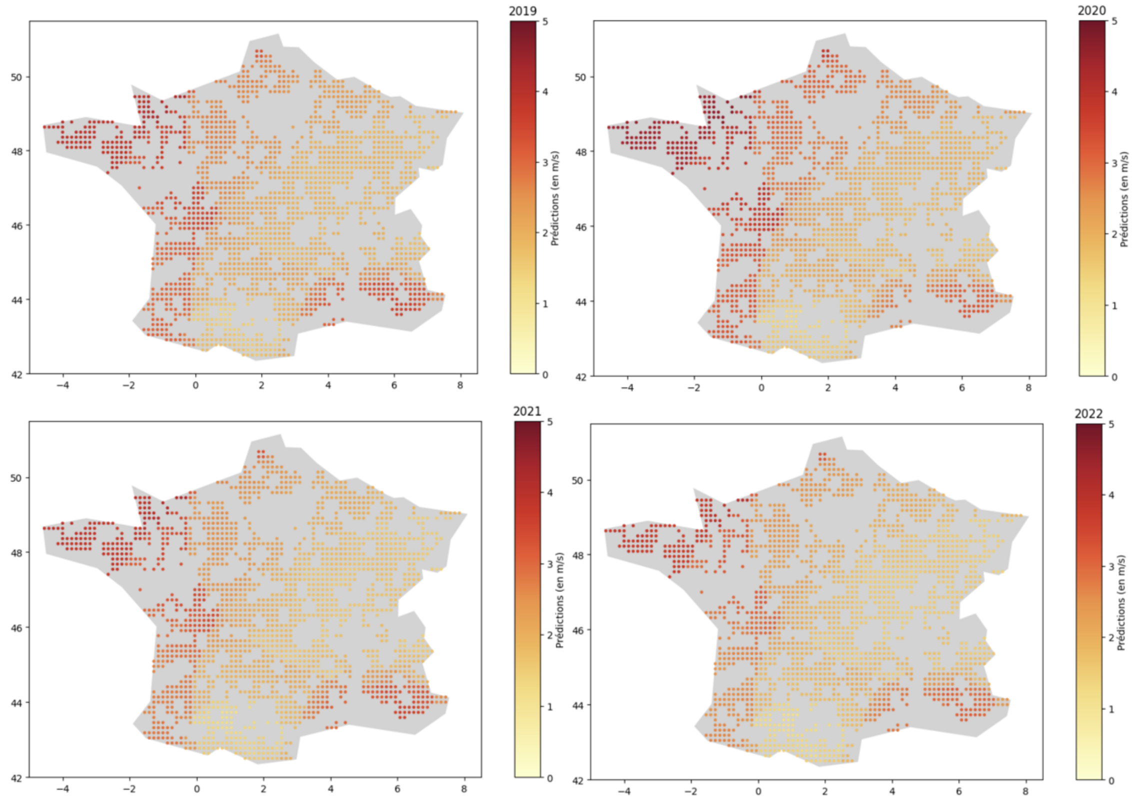

Figure 18: Comparison of wind speed predictions from 2019 to 2022

However, it is important to note that this study requires predicting wind speed on spatial dimensions as well as temporal dimensions. However, we found it extremely difficult to make wind speed predictions for time horizons beyond a few days. Anticipating wind speed for the years to come would have been complex and unreliable. Indeed, meteorology experts, such as Richard Harvey [8], agree that no prediction can "be reliable beyond a certain threshold of time". He sets this threshold at 5 daysdue to the "chaotic" behavior of the atmosphere. In common language, reference is often made to the "butterfly effect", where a butterfly flapping its wings in Brazil may eventually trigger a hurricane in the Philippines. Even slight differences can trigger a domino effect in the short or long term, influencing the atmosphere and, consequently, the ability to make wind predictions.

To go around this difficulty, we hypothesized that wind speed will remain relatively constant in the years to come, and we focused on the spatial dimension. This hypothesis is reinforced by the observation that over the past four years, wind speed predictions showed some similarity from one year to another.

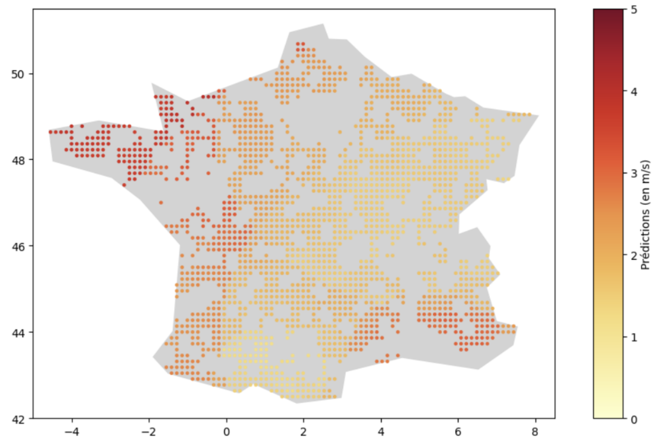

Figure 19: Prediction of wind speed in 2022

6.4 Estimation of energy produced

Now that we have quantified the available energy source, namely the energy associated with wind speed across France, we can estimate the electrical power produced, in Watts, by a wind turbine at these locations.

The kinetic energy of the wind, determined by its mass and velocity, is expressed by the formula $E_c = \frac{1}{2} \cdot \rho \cdot V^2$, where ρ is the air mass. Wind turbines exploit this kinetic energy by slowing down the wind through the surface of their rotor. The air flow passing through the wind turbine (in kg per second) is defined by $V \cdot S \cdot \rho$, where:

- V is the wind speed in meters per second
- S is the surface covered by the blades, forming a circle with an area of $\pi \cdot R^2$
- ρ is the air density in kg/m^3

Finally, by combining these two formulas [9], the power calculation can be simplified to:

$$P = \frac{1}{2} \cdot \rho \cdot S \cdot V^3$$

where P represents the power in Watts.

The amount of energy recovered through the rotor is proportional to its surface area, evolving exponentially depending on the radius of the blades: if the radius doubles, the power is multiplied by 4. It is also proportional to the wind speed cubed, which implies that if the wind speed doubles, the power is multiplied by 8. Hence, the importance of placing wind turbines in windy sites.

We know that the air density depends on temperature, humidity, and atmospheric pressure. Depending on these parameters, variations of 20% in air density and therefore in wind power can be obtained. For example, at sea level, at -10°C, one cubic meter of air will weigh 1.341 kg, while at 30°C, it will weigh only 1.164 kg. Therefore, we considered an average value of 1.2 kg/m^3. We evaluated the installation of an average wind turbine with a radius of 40 meters, which represents a surface covered by the blades of approximately 5,000 m^2.

The following map illustrates the total annual power at each point in France. It was obtained by summing the daily power obtained by applying the formula to the daily wind speed forecasts for the year 2022.

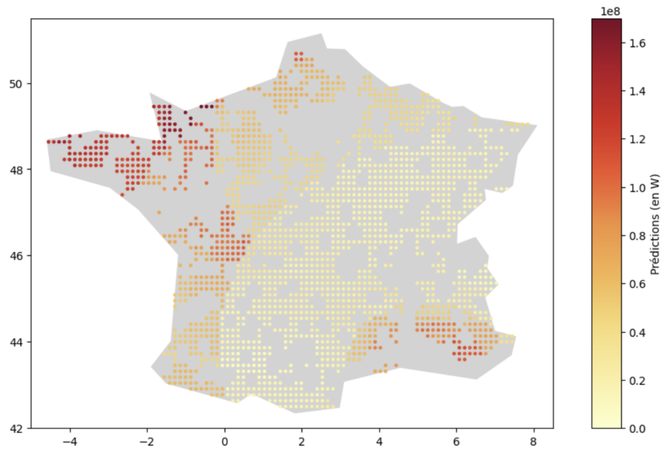

Figure 20: Map of 2022 predictions of total annual power (in W)

The results obtained are similar to those illustrating wind speed: the power of the wind turbines is, on average, higher in the Northwest and Southeast regions. We restricted the possible locations for the installation of wind turbines to points where the total annual power exceeds 60 MWh, which corresponds to the power at the 3rd quartile.

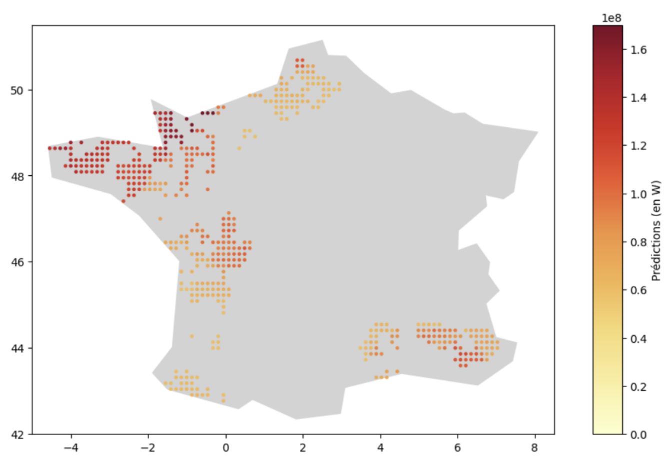

Figure 21: Map of Locations with Power > 60 MWh

6.5 Energy Demand by French Municipality

Wind turbines should be positioned as close as possible to electricity consumption sources to optimize energy distribution and minimize losses related to electricity transmission and the need for storage. That's why we are now focusing on annual electricity consumption per municipality. Our approach is to install wind turbines closer to municipalities with high energy demand. To do this, we used a database from the ORE & Electricity and Gas Network Managers Agency [2] which lists annual consumption per municipality from 2011 to 2021. We calculated the average annual consumption over these 11 years to target the most energy-consuming municipalities. Subsequently, we focused on the top 1% of municipalities with the highest electricity consumption (over 200,000 MWh per year), thus grouping 340 municipalities.

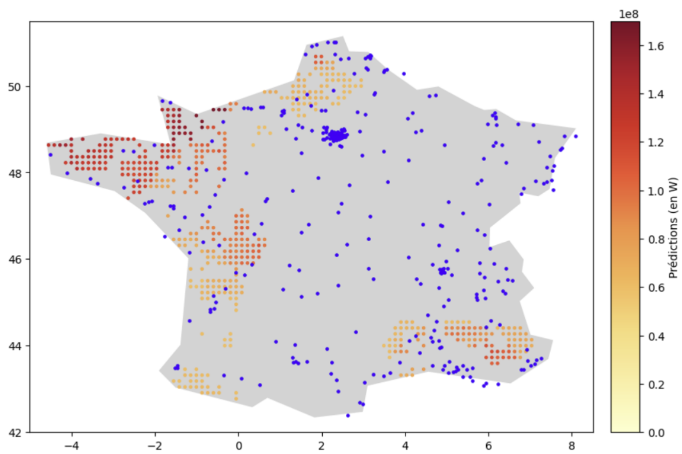

Figure 22: Map of Locations with Power > 60 MWh (in red) and Communes with Highest Consumption (in blue)

It is important to note that energy demand is uniformly distributed throughout the French territory. Therefore, to avoid losses related to energy transport, it is necessary to judiciously distribute the locations of wind turbines across the entire territory. To do so, we developed an algorithm to select the top 10 locations that minimize the cumulative distance between high-energy-demand cities and wind turbines. We used the *scipy.spatial* library to calculate the distance matrix between the geographical coordinates of the blue points (representing high-energy-demand cities) and the red points (potential locations for wind turbines). The issue with this method is that it is difficult to test all possible combinations of 10 wind turbines:

$$C(473, 10) = \frac{473!}{10!(473 - 10)!}$$

Therefore, we restricted our possibilities to 1,000,000 random combinations. Ultimately, the top 10 locations for wind turbines are illustrated in the figure below.

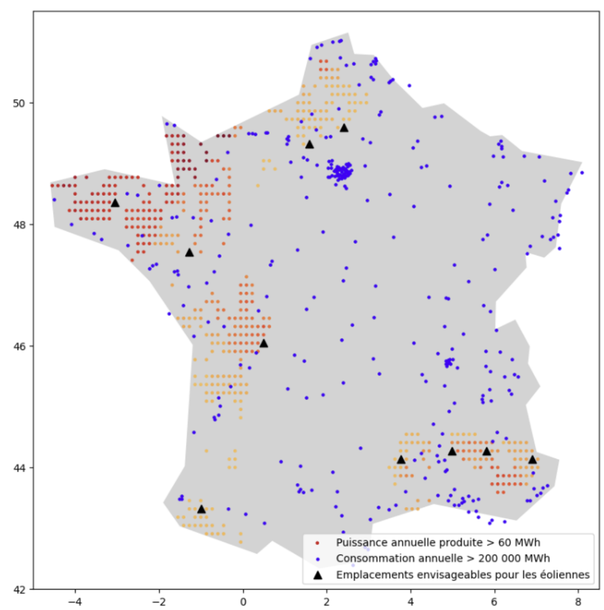

Figure 23: Best Locations for Wind Turbines

These locations were selected taking into account several essential criteria. Firstly, wind power was rigorously evaluated, ensuring energy production exceeding 60 MWh. Additionally, to respect nearby residences, each location is situated at a safe distance of more than 20 kilometers from major cities (cities with more than 10,000 inhabitants). Finally, these locations optimize energy distribution by considering the energy demand of municipalities. They are positioned to minimize distances between cities with high energy demand and wind turbines. This approach allowed for reconciling energy efficiency, local environmental respect, and response to regional energy needs.

7 Conclusion

Overall, in our analysis, we saw the evolution at regional and national levels of wind turbine capacity. We noticed two different trends. First, regarding wind power generation, we observed fluctuations, emphasizing the seasonal and cyclical nature of wind energy displaying that more energy is produced in winter. Second, there is an overall increasing trend over the years, mirroring the capacity analysis where we saw that more and more wind turbines have been installed over the years.

Then, to determine the most promising sites, we sought to predict the potential energy generated by the wind farm based on its location. However, to do so, we first needed to make wind speed predictions across France. We thus explored various models such as kriging, linear regression, and an XGBoost model. The results obtained with linear regression were not convincing. Although Kriging produced promising results for monthly predictions, we ultimately opted for the XGBoost model due to its superior performance in daily predictions. This allowed us to establish an initial list of potential locations for wind farm deployment. These locations were selected by ensuring sufficient wind stability and power to ensure the operation of wind farms.

Our study then narrowed down to locations close enough to urban areas to avoid electrical energy losses associated with transportation. However, we made sure not to place them too close to urban areas to avoid noise and visual disturbances for residents. Thus, we identified 10 potential positions: the proposed sites often being located near the coastal areas. Near the Mediterranean coasts, we found two locations in the Occitanie region, and two others located in the Provence-Alpes-Côte d'Azur region. Near the Atlantic Coast, we found three locations: one in Brittany, one in Pays de la Loire, and one further south in Nouvelle-Aquitaine. Two additional locations were positioned at the north of the Île-de-France region.

However, one crucial consideration is that wind forecasting is tied to frequent variations in the atmosphere. Due to these changes, the wind forecasting model heavily relies on the accuracy of available atmospheric data. The accuracy of our predictions could be improved by continuously integrating additional daily data. This will better anticipate short-term changes, thus making predictions more reliable and suitable for the near future.

This study provides a good foundation and starting point for future studies, offering opportunities to refine the prediction model and stay up to date on what is happening with wind energy. This is important for France's goal of achieving carbon neutrality by 2050 and sustainable energy practices.

References

[1] Vioux Daniel. Météorologie, circulation générale de l'atmosphere. https://www.lavionnaire.fr/MeteoCirculation.php, 2018.

[2] Agence ORE & Gestionnaires de réseaux électricité et gaz. Consommation annuelle d'électricité et gaz par commune et par secteur d'activité. https://opendata.agenceore.fr/explore/dataset/conso-elec-gaz-annuelle-par-secteur-dactivite-agregee-commune/information/, 2021.

[3] EDF. Le fonctionnement d'une éolienne. https://www.edf.fr/groupe-edf/espaces-dedies/jeunes-enseignants/pour-les-jeunes/lenergie-de-a-a-z/produire-de-lelectricite/le-fonctionnement-dune-eolienne#:~:text=Le%20rotor%20entra%C3%AEne%20un%20axe,de%20la%20puissance%20du%20vent, 2015.

[4] Jean Michel Floch. Chapitre 5 : Géostatistique. https://www.insee.fr/fr/statistiques/fichier/3635442/imet131-i-chapitre-5.pdf.

[5] Météo France. Observation météorologique historiques france (synop). https://public.opendatasoft.com/explore/dataset/donnees-synop-essentielles-omm/table/?flg=fr-fr&sort=date&q.timerange.date=date:%5B2017-12-31T23:00:00Z+TO+2023-01-01T22:59:59Z%5D&dataChart=eyJxdWVyaWVzIjpbeyJjaGFydHMiOlt7InR5cGUiOiJjb2x1bW4iLCJmdW5jIjoiQVZHIiwieUF4aXMiOiJOYyIsInNjaWVud3D&location=6,43.2852,5.37231&basemap=jawg.light, 2023.

[6] René Fury and Daniel Joly. Interpolation spatiale à maille fine des températures journalières. https://www.researchgate.net/publication/271094123_Interpolation_spatiale_a_maille_fine_des_temperatures_journalieres, 2013.

[7] gouv.fr. geo.api. https://geo.api.gouv.fr/decoupage-administratif/communes, 2021.

[8] Richard Harvey. La prévision météorologique : limites et possibilités. https://www.solutions-mesonet.org/la-prevision-meteorologique-limites-et-possibilites-partie-1/, 2021.

[9] Page Jaune. Puissance éolienne. https://eolienne.pagesjaunes.fr/astuce/voir/352953/puissance-eolienne, 2023.

[10] Changyeon Lee. Long-term wind speed interpolation using anisotropic regression kriging with regional heterogeneous terrain and solar insolation in the united states.

https://www-sciencedirect-com.gorgone.univ-toulouse.fr/science/article/pii/S2352484721014323, 2021.

[11] Aurore Dupré Riwal Plougonven Rebeca Doctors Lishan Liao Mathilde Mougeot Aurélie Fischer Naveen Goutham, Bastien Alonzo and Philippe Drobinski. Using machine-learning methods to improve surface wind speed from the outputs of a numerical weather prediction model. file:///C:/Users/PE151630/Downloads/machinelearningmethodswind.pdf, 2021.

[12] M.A.Baseer S.Rehman and L.M. Alhems. Gis-based multi-criteria wind farm site selection methodology. https://scindeks-clanci.ceon.rs/data/pdf/1451-2092/2020/1451-20922004855R.pdf, 2020.

[13] Sénat. Séance du 3 novembre 2022. https://www.senat.fr/seances/s202211/s20221103/s20221103014.html, 2022.

[14] Ma terre. Éolien terrestre. https://www.mtaterre.fr/articles/comment-ca-marche-lenergie-eolienne/, 2023.

Appendices

Appendix 1: Variables of the SYNOP dataset

Variable	Description
ID OMM station	Identification code for the station
Date	Date of observation
Pression au niveau mer	Sea level pressure
Variation de pression en 3 heures	Pressure change in the last 3 hours
Type de tendance barométrique	Type of barometric tendency
Direction du vent moyen 10 mn	Average wind direction over 10 minutes
Vitesse du vent moyen 10 mn	Average wind speed over 10 minutes
Température	Temperature
Point de rosée	Dew point
Humidité	Humidity
Visibilité horizontale	Horizontal visibility
Temps présent	Present weather
Temps passé 1	Past weather 1
Temps passé 2	Past weather 2
Nebulosité totale	Total cloud cover
Nébulosité des nuages de l'étage inférieur	Cloud cover of low-level clouds
Hauteur de la base des nuages de l'étage inférieur	Height of base of low-level clouds
Type des nuages de l'étage inférieur	Type of low-level clouds
Type des nuages de l'étage moyen	Type of mid-level clouds
Type des nuages de l'étage supérieur	Type of high-level clouds
Pression station	Station pressure
Niveau barométrique	Barometric altitude
Géopotentiel	Geopotential
Variation de pression en 24 heures	Pressure change in the last 24 hours
Température minimale sur 12 heures	Minimum temperature over 12 hours
Température minimale sur 24 heures	Minimum temperature over 24 hours
Température maximale sur 12 heures	Maximum temperature over 12 hours
Température maximale sur 24 heures	Maximum temperature over 24 hours
Température minimale du sol sur 12 heures	Minimum ground temperature over 12 hours
Méthode de mesure Température du thermomètre mouillé	Method of measuring wet-bulb temperature
Température du thermomètre mouillé	Wet-bulb temperature
Rafale sur les 10 dernières minutes	Wind gusts in the last 10 minutes
Rafales sur une période	Wind gusts over a period
Période de mesure de la rafale	Period of wind gust measurement
État du sol	Ground state
Hauteur totale de la couche de neige, glace, autre au sol	Total height of snow, ice, or other on the ground
Hauteur de la neige fraîche	Height of fresh snow
Période de mesure de la neige fraîche	Period of fresh snow measurement
Précipitations dans la dernière heure	Precipitation in the last hour
Précipitations dans les 3 dernières heures	Precipitation in the last 3 hours
Précipitations dans les 6 dernières heures	Precipitation in the last 6 hours
Précipitations dans les 12 dernières heures	Precipitation in the last 12 hours
Précipitations dans les 24 dernières heures	Precipitation in the last 24 hours
Phénomène spécial 1	Special phenomenon 1
Phénomène spécial 2	Special phenomenon 2
Phénomène spécial 3	Special phenomenon 3
Phénomène spécial 4	Special phenomenon 4
Nébulosité couche nuageuse 1	Cloud cover layer 1
Type nuage 1	Cloud type 1
Hauteur de base 1	Base height 1
Nébulosité couche nuageuse 2	Cloud cover layer 2
Type nuage 2	Cloud type 2
Hauteur de base 2	Base height 2

Variable	Description
Nébulosité couche nuageuse 3	Cloud cover layer 3
Type nuage 3	Cloud type 3
Hauteur de base 3	Base height 3
Nébulosité couche nuageuse 4	Cloud cover layer 4
Type nuage 4	Cloud type 4
Hauteur de base 4	Base height 4
Coordonnées	Coordinates
Nom	Name
Type de tendance barométrique.1	Type of barometric tendency 1
Temps passé 1.1	Past weather 1.1
Temps présent.1	Present weather 1
Température (°C)	Temperature (°C)
Température minimale sur 12 heures (°C)	Minimum temperature over 12 hours (°C)
Température minimale sur 24 heures (°C)	Minimum temperature over 24 hours (°C)
Température maximale sur 12 heures (°C)	Maximum temperature over 12 hours (°C)
Température maximale sur 24 heures (°C)	Maximum temperature over 24 hours (°C)
Température minimale du sol sur 12 heures (en °C)	Minimum ground temperature over 12 hours (in °C)
Latitude	Latitude
Longitude	Longitude
Altitude	Altitude
communes (name)	Name of the locality
communes (code)	Code of the locality
EPCI (name)	Name of the Public Establishment of Inter-Municipal Cooperation
EPCI (code)	Code of the Public Establishment of Inter-Municipal Cooperation
department (name)	Name of the department
department (code)	Code of the department
region (name)	Name of the region
region (code)	Code of the region
$mois\_de\_l_{a}nnee$	Month of the year

Appendix 2: Presentation of the different codes

- The "Analysis of Wind Turbines in France" script contains the data analysis of the Wind Turbines in France. It includes several key steps, from cleaning the input data to the detailed analysis and all the graphs.

- The "ML prediction" script encompasses the code dedicated to using the XGBoost algorithm for making predictions. It includes several key steps, from cleaning the input data required for model training, to creating the XGBoost model itself, formatting the database to be predicted, and making predictions.

- The "energy demand" script is designed to determine the optimal locations for wind turbines based on energy needs. To use it, you need a database listing cities with high energy consumption, as well as a database of potential wind turbine locations. The algorithm relies on distance optimization, seeking to identify the 10 best locations for wind turbines to meet specific energy demand.

- The "LinearRegression" script uses SYNOP data to create a linear regression where the dependent variable is wind speed and the independent variables are altitude, longitude, latitude, and indicators for year, month, day, and time of measurement. This code also creates the map with SYNOP station positions.

- The "Maps" script is designed to visualize potential wind turbine locations in France using the GeoPandas library. It starts with the grid plot, then removes major cities before placing wind turbines based on wind speed and annual commune consumption.

- The "KrigingGrid" script generates a grid covering the entire France. The user can determine the size of the grid cells. The number of generated points is automatically calculated. In this notebook, you will also find the necessary codes to obtain wind speed prediction for a given geographical location using ordinary kriging as well as kriging with regression.

Appendix 3: Results of the linear regression

	coef	std err	t	P> |t|	[0.025	0.975]
const	3.2995	0.084	39.470	0.000	3.136	3.463
month_2	0.3012	0.018	16.573	0.000	0.266	0.337
month_3	0.2675	0.018	14.861	0.000	0.232	0.303
month_4	-0.0012	0.032	-0.038	0.970	-0.065	0.062
month_5	-0.0743	0.032	-2.296	0.022	-0.138	-0.011
month_6	-0.4094	0.032	-12.614	0.000	-0.473	-0.346
month_7	-0.4024	0.032	-12.422	0.000	-0.466	-0.339
month_8	-0.4703	0.032	-14.525	0.000	-0.534	-0.407
month_9	-0.4359	0.032	-13.429	0.000	-0.500	-0.372
month_10	-0.0265	0.030	-0.889	0.374	-0.085	0.032
month_11	-0.3289	0.018	-18.385	0.000	-0.364	-0.294
month_12	0.0663	0.018	3.743	0.000	0.032	0.101
year_2019	0.1786	0.012	15.496	0.000	0.156	0.201
year_2020	0.2427	0.012	21.072	0.000	0.220	0.265
year_2021	0.0489	0.012	4.235	0.000	0.026	0.071
year_2022	0.0105	0.012	0.909	0.363	-0.012	0.033
year_2023	1.2006	0.156	7.675	0.000	0.894	1.507
day_2	0.0259	0.028	0.912	0.362	-0.030	0.082
day_3	-0.0753	0.028	-2.648	0.008	-0.131	-0.020
day_4	-0.0395	0.028	-1.389	0.165	-0.095	0.016
day_5	-0.0880	0.028	-3.094	0.002	-0.144	-0.032
day_6	-0.0891	0.028	-3.140	0.002	-0.145	-0.033
day_7	-0.0108	0.028	-0.379	0.705	-0.066	0.045
day_8	-0.1983	0.028	-6.978	0.000	-0.254	-0.143
day_9	-0.0081	0.028	-0.286	0.775	-0.064	0.048
day_10	-0.0079	0.028	-0.277	0.782	-0.064	0.048
day_11	-0.1168	0.028	-4.111	0.000	-0.173	-0.061
day_12	-0.2061	0.028	-7.263	0.000	-0.262	-0.150
day_13	0.0576	0.028	2.023	0.043	0.002	0.113
day_14	0.0170	0.028	0.598	0.550	-0.039	0.073

	coef	std err	t	P> |t|	[0.025	0.975]
day_15	-0.0125	0.028	-0.442	0.659	-0.068	0.043
day_16	-0.2348	0.028	-8.250	0.000	-0.291	-0.179
day_17	-0.1345	0.028	-4.738	0.000	-0.190	-0.079
day_18	-0.2539	0.028	-8.924	0.000	-0.310	-0.198
day_19	-0.2162	0.028	-7.612	0.000	-0.272	-0.161
day_20	-0.0272	0.028	-0.957	0.339	-0.083	0.028
day_21	-0.0504	0.028	-1.776	0.076	-0.106	0.005
day_22	-0.1307	0.028	-4.594	0.000	-0.187	-0.075
day_23	-0.2259	0.028	-7.952	0.000	-0.282	-0.170
day_24	-0.2433	0.028	-8.556	0.000	-0.299	-0.188
day_25	-0.2138	0.028	-7.517	0.000	-0.270	-0.158
day_26	-0.1490	0.028	-5.241	0.000	-0.205	-0.093
day_27	0.0372	0.028	1.309	0.190	-0.019	0.093
day_28	0.1291	0.028	4.537	0.000	0.073	0.185
day_29	0.0227	0.029	0.783	0.434	-0.034	0.079
day_30	-0.2892	0.029	-9.954	0.000	-0.346	-0.232
day_31	-0.2032	0.033	-6.111	0.000	-0.268	-0.138
hour_02	-0.5876	0.034	-17.488	0.000	-0.653	-0.522
hour_04	-0.0365	0.023	-1.606	0.108	-0.081	0.008
hour_05	-0.7144	0.034	-21.311	0.000	-0.780	-0.649
hour_07	-0.0045	0.023	-0.197	0.844	-0.049	0.040
hour_08	-0.6625	0.034	-19.766	0.000	-0.728	-0.597
hour_10	0.3144	0.023	13.840	0.000	0.270	0.359
hour_11	0.1620	0.034	4.831	0.000	0.096	0.228
hour_13	1.0062	0.023	44.326	0.000	0.962	1.051
hour_14	0.8525	0.034	25.424	0.000	0.787	0.918
hour_16	0.9651	0.023	42.545	0.000	0.921	1.010
hour_17	1.0409	0.034	31.059	0.000	0.975	1.107
hour_19	0.2279	0.023	10.050	0.000	0.183	0.272
hour_20	0.3793	0.034	11.319	0.000	0.314	0.445
hour_22	0.0939	0.023	4.141	0.000	0.049	0.138

	coef	std err	t	P> |t|	[0.025	0.975]
hour_23	-0.4163	0.034	-12.412	0.000	-0.482	-0.351
latitude	0.0193	0.002	11.600	0.000	0.016	0.023
longitude	-0.0716	0.001	-57.402	0.000	-0.074	-0.069
altitude	-0.0016	1.87e-05	-84.674	0.000	-0.002	-0.002

Appendix 4: Monthly Wind Speed Predictions for 2022

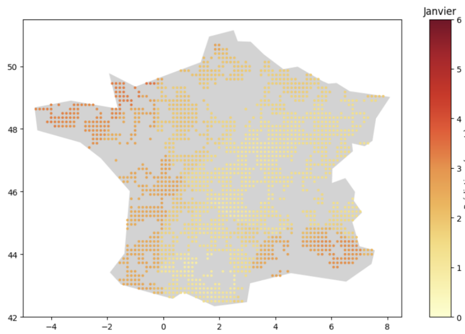

Figure 24: January 2022 Wind Speed Prediction

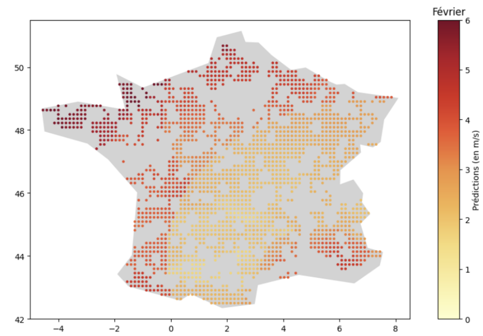

Figure 25: February 2022 Wind Speed Prediction

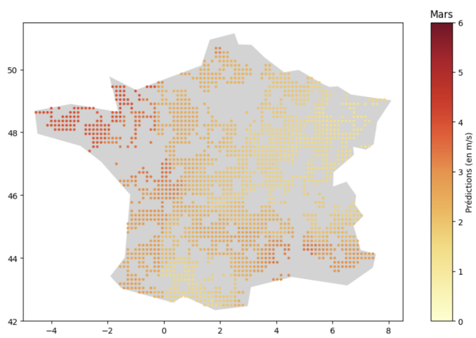

Figure 26: March 2022 Wind Speed Prediction

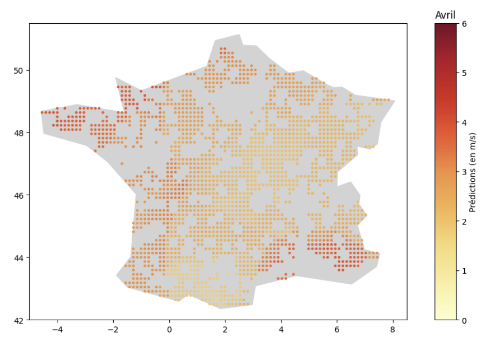

Figure 27: April 2022 Wind Speed Prediction

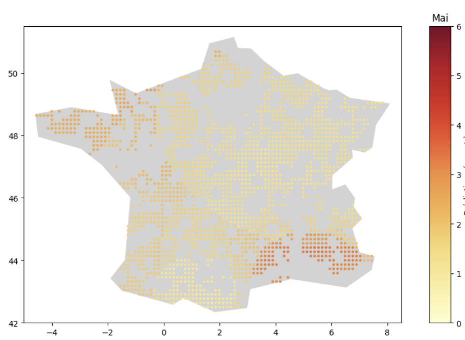

Figure 28: May 2022 Wind Speed Prediction

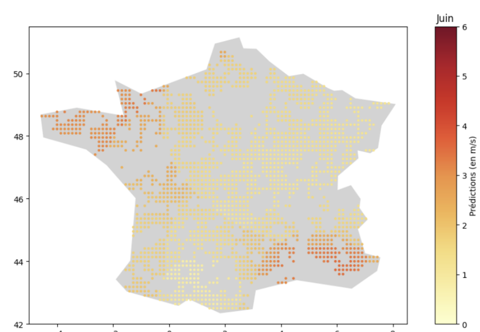

Figure 29: June 2022 Wind Speed Prediction

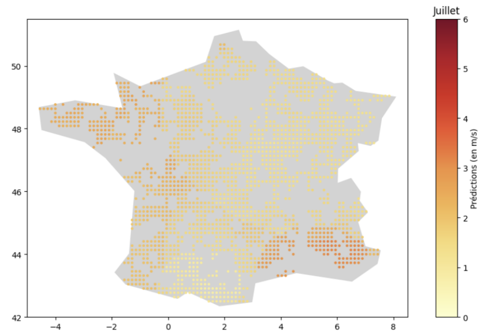

Figure 30: July 2022 Wind Speed Prediction

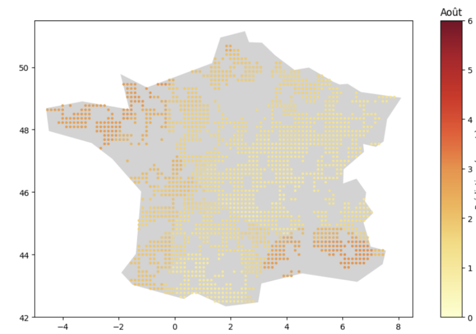

Figure 31: August 2022 Wind Speed Prediction

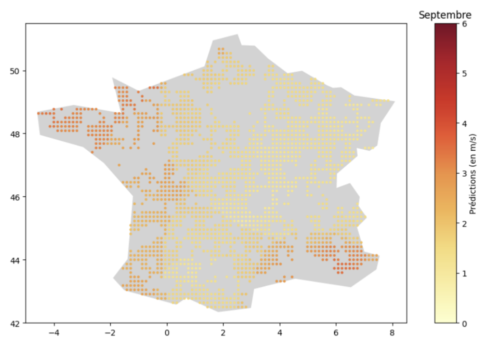

Figure 32: September 2022 Wind Speed Prediction

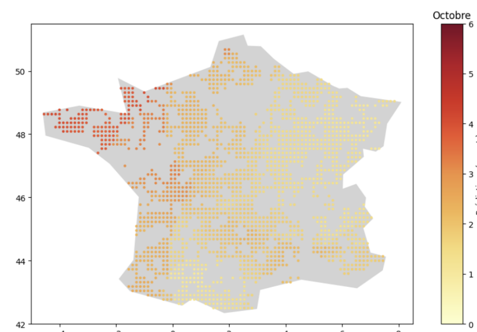

Figure 33: October 2022 Wind Speed Prediction

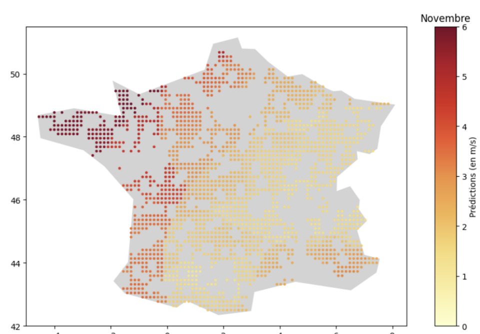

Figure 34: November 2022 Wind Speed Prediction

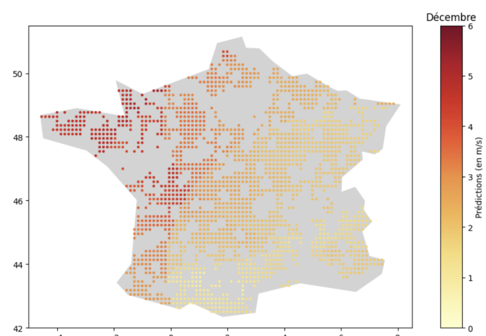

Figure 35: December 2022 Wind Speed Prediction